HHS Public Access

Author manuscript

Brain Imaging Behav. Author manuscript; available in PMC 2015 December 01.

Published in final edited form as:

Brain Imaging Behav. 2015 December ; 9(4): 868–877. doi:10.1007/s11682-014-9349-1.

White matter abnormalities of microstructure and physiological noise in schizophrenia

Hu Cheng, **Sharlene D. Newman**, **Jerillyn S. Kent**, **Amanda Bolbecker**, **Mallory J. Klaunig**, **Brian F. O'Donnell**, **Aina Puce**, and **William P. Hetrick**

Department of Psychological and Brain Sciences, Indiana University, Bloomington, IN 47405, USA

Hu Cheng: hucheng@indiana.edu

Abstract

White matter abnormalities in schizophrenia have been revealed by many imaging techniques and analysis methods. One of the findings by diffusion tensor imaging is a decrease in fractional anisotropy (FA), which is an indicator of white matter integrity. On the other hand, elevation of metabolic rate in white matter was observed from positron emission tomography (PET) studies. In this report, we aim to compare the two structural and functional effects on the same subjects. Our comparison is based on the hypothesis that signal fluctuation in white matter is associated with white matter functional activity. We examined the variance of the signal in resting state fMRI and found significant differences between individuals with schizophrenia and non-psychiatric controls specifically in white matter tissue. Controls showed higher temporal signal-to-noise ratios clustered in regions including temporal, frontal, and parietal lobes, cerebellum, corpus callosum, superior longitudinal fasciculus, and other major white matter tracts. These regions with higher temporal signal-to-noise ratio agree well with those showing higher metabolic activity reported by studies using PET. The results suggest that individuals with schizophrenia tend to have higher functional activity in white matter in certain brain regions relative to healthy controls. Despite some overlaps, the distinct regions for physiological noise are different from those for FA derived from diffusion tensor imaging, and therefore provide a unique angle to explore potential mechanisms to white matter abnormality.

Keywords

Physiological noise; Schizophrenia; White matter; Resting state fMRI

Correspondence to: Hu Cheng, hucheng@indiana.edu.

Electronic supplementary material: The online version of this article (doi:10.1007/s11682-014-9349-1) contains supplementary material, which is available to authorized users.

Conflicts of interest Hu Cheng, Sharlene D. Newman, Jerillyn S. Kent, Amanda Bolbecker, Mallory J. Klaunig, Brian F. O'Donnell, Aina Puce, and William P. Hetrick declare that they have no conflicts of interest.

Informed consent All procedures followed were in accordance with the ethical standards of the responsible committee on human experimentation (institutional and national) and with the Helsinki Declaration of 1975, and the applicable revisions at the time of the investigation. Informed consent was obtained from all patients for being included in the study.

Introduction

Schizophrenia is a severe psychiatric disorder that is believed to be affected by many factors including genetics, volumetric brain abnormalities, and the integrity of neuronal circuits (Benes 2000; Honea et al. 2005; Ripke et al. 2013; Shenton et al. 2001). Studies have suggested that alterations in the brain's white matter are key to understanding schizophrenia (Davis et al. 2003; Karlsgodt et al. 2009). White matter abnormalities in individuals with schizophrenia (SZ) have primarily been demonstrated by diffusion tensor imaging (DTI) (Camchong et al. 2011; Kubicki et al. 2007; White et al. 2011). These studies have reported decreased fractional anisotropy and increased diffusivity in frontal, parietal, occipital, and temporal lobes, as well as abnormalities within the fiber bundles connecting these regions (e.g., uncinate fasciculus) (Kubicki et al. 2007; Lee et al. 2013).

For the last two decades, advances in magnetic resonance technology have engendered many new tools for exploring brain anatomy and function. In an attempt to understand white matter abnormalities from a different perspective, researchers have adopted many other MR techniques besides diffusion tensor imaging. For instance, voxel-based morphometry on T1-weighted anatomical images reveals structural differences in schizophrenia (Honea et al. 2005); mapping of T1 and T2 relaxation time that is related to molecular structure shows that schizophrenia is associated with a longer T2 in white matter (Du et al. 2012; Pfefferbaum et al. 1999); magnetization transfer ratio can serve as an index of myelination integrity (Du et al. 2013); PET and magnetic resonance spectroscopy provides metabolic information (Buchsbaum et al. 2007; Du et al. 2012); and resting state functional connectivity demonstrates wide disruption of functional connectivity between brain regions in SZ (Lynall et al. 2010). Aggregated data from all of these techniques have generated a more comprehensive picture of white matter microstructure and function, as well as the white matter structural and functional abnormalities in schizophrenia.

Among those findings of structural and functional abnormalities in white matter, two effects are wide spread. Structurally, it is decreased fractional anisotropy; functionally, it is elevated metabolic rate. Higher glucose metabolic rates were found in white matter in SZ using ^{18}F Fludeoxyglucose (FDG) PET (Buchsbaum et al. 2007). SZ patients showed higher relative metabolic rates in the frontal white matter, corpus callosum, superior longitudinal fasciculus, and white matter core of the temporal lobe. Elevated activity in white matter was most pronounced in the center of large white matter tracts, especially in the frontal regions and the internal capsule (Buchsbaum et al. 2007). Perfusion studies using arterial spin labeling also showed that cerebral blood flow increases in some white matter areas while it decreases in some cortical regions (Pinkham et al. 2011). Together these findings suggest that examining functional activity in white matter may prove to be important in understanding some of the altered functions in SZ. The feature of wide-spread structural and functional abnormalities also suggest the need for further investigation of the relationship between the two.

It is important to understand whether structural and functional brain changes are associated in schizophrenia and, more importantly, whether one is mediated by the other. This issue was partly addressed by exploring the amplitude of low-frequency fluctuations in resting

state fMRI and volumetric changes of gray matter (Ren et al. 2013) in specific cortical regions. A dissociation of anatomical and functional deficits was observed in gray matter for first-episode schizophrenia individuals. Similarly, we can examine white matter abnormalities using diffusion tensor imaging and signal fluctuation in resting state fMRI. In functional MRI, the vascular signal change is coupled with neurophysiological activity. The blood oxygenation level dependent (BOLD) contrast arises from the metabolic linked changes in cerebral blood flow, oxygenation, and blood volume (Kim et al. 1999; Ogawa et al. 1990). Resting state fMRI acquires data when no specific task is being performed. When there is no specific task, the brain still needs to maintain normal metabolism (Raichle and Gusnard 2002). Recent discovery of resting state functional connectivity derived from the correlation of time courses between brain regions indicates the functional aspect of MRI signal fluctuation. In general, the signal variation or noise in an MRI image can be decomposed into thermal noise from the subject and scanner electronics, other system-related noise due to imperfections in different scanner subsystems such as the gradient and shim, and physiological noise from brain/body metabolic and physiological activity (Kruger and Glover 2001). Physiological noise arises from fluctuations in basal cerebral metabolism ($CMRO_2$), cerebral blood flow (CBF), and cerebral blood volume (CBV), and also from vascular variations coupled with cardiac and respiratory activity, motion from subtle brain pulsations as a function of the cardiac cycle, and magnetic field modulations. As a result, lower regional physiological noise has been found in patients with ischemic stroke due to lower blood flow (Wang et al. 2008).

The distribution of noise is not spatially uniform in the brain. Thermal noise and system noise are almost identical in gray and white matter, but physiological noise is much larger in gray matter. On one hand, gray matter has higher functional activity reflected by higher blood flow, higher oxygenation, and higher blood volume, as confirmed by positron emission tomography (PET) studies and MRI perfusion studies (Buchsbaum et al. 2007; Pinkham et al. 2011). On the other hand, gray matter has more vasculature than white matter, resulting in larger fluctuations from cardiac and respiratory functions. On average, physiological noise in gray matter is about twice that in white matter (Kruger and Glover 2001). This number is very close to the ratio of CBF, or $CMRO_2$, between gray matter and white matter for young adults, which is 2.07 and 2.16, respectively (Pantano et al. 1984).

Given that a growing body of evidence shows functional activation in white matter and white matter connectivity (Ding et al. 2013; Gawryluk et al. 2014), we believe that the signal fluctuation in white matter also conveys functional information, just as that in gray matter. Hence we attempted to investigate functional abnormalities in SZ by examining physiological noise and further compare it directly with FA differences derived from diffusion tensor imaging. The relation between white matter diffusion anisotropy and functional activity was first investigated by Buchsbaum et al. using PET imaging, revealing a correlation between changes in metabolic rate in the prefrontal cortex and striatum in SZ patients (Buchsbaum et al. 1998). As white matter is composed of more than axons (e.g., glial cells that are responsible for the creation of myelin) the metabolism taking place in white matter may be linked to the broader integrity of white matter tracts. Therefore, relating this functional activity to diffusion measures of white matter may be informative about the neurobiology of schizophrenia. There is also one advantage of focusing on the analysis of

white matter. The source of physiological noise in white matter, compared to gray matter, is significantly less affected by cardiac pulsation and respiration, which are not directly related to neuronal activity.

Methods

Subject recruitment

29 SZs (8 female, mean age 36.7± 9.9 years) and 36 non-psychiatric controls (NCs) (18 female, mean age 29.3±6.5 years) were recruited and completed the study protocol. However, some subjects were excluded (10 SZs and 7 NCs) from this study due to imaging problems and the stringent criterion applied to detect excessive head motion. Remaining subjects were 16 SZs (5 female, mean age 31.6± 9.1 years) and 29 NCs (15 female, 29.6±9.8). Diagnosis was determined using the Structured Clinical Interview for the DSM-IV Axis I Disorders (SCID-I) (First et al., 2002) and medical chart review. The SCID-I for non-patients was used to confirm that there was no history of Axis I disorders in the NCs. Current drug or alcohol abuse or dependence or a loss of consciousness lasting more than 5 min were exclusionary criteria for all participants. All subjects passed a urine screening for illicit substances at the time of the scan.

MRI scans

Subjects were scanned using a Siemens TIM Trio 3 T MRI scanner using a 32-channel coil. The high resolution (1 mm^3) anatomical scan was performed with the 3D MP-RAGE sequence (matrix=256×256, FOV=256×256 mm, TE/TR=2.67/1800 ms, TI=900 ms), followed by a DTI scan (matrix=128 × 128; FOV = 256×256 mm; TE/TR=77/8300 ms; 68 transversal slices with 2 mm thickness; 48 diffusion directions with gradients b=1000 s/mm^2, and 8 samplings at b=0). The final scan was a resting fMRI scan performed with an EPI sequence (TR/TE=2500/30 ms, FOV=220 mm, 128×128 matrix, iPAT2, 200 volumes). During the resting scan, subjects rested with eyes closed for approximately 9 min. Both DTI and EPI scans used the parallel imaging technique GRAPPA with an acceleration factor of 2 (iPAT2).

Motion analysis

Functional images were motion corrected using MCFLIRT in FSL (http://www.fmrib.ox.ac.uk/fsl/). Since subject head movement can introduce significant variance into fMRI time series, a careful examination of the motion characteristics of each subject was carried out by examining the transformation parameters of the MCFLIRT output. For each subject, we compared relative motion of all volumes with respect to the 100th volume (the middle one). All volumes with translation motion>0.5 mm and rotational motion>1° were excluded. If a subject had less than 100 volumes remaining, the subject was excluded from the study. In the end, a new quantity was introduced to quantify the total translational motion or total rotational motion, defined as the root mean of volume-volume variance of translation and rotation respectively (Van Dijk et al. 2012):

$$Trans(Rot)=\frac{1}{N-1}\sum_{i=1}^{N-1}\sqrt{(a_{i+1}-a_i)^2+(b_{i+1}-b_i)^2+(c_{i+1}-c_i)^2} \quad (1)$$

where N is the number of volumes and a, b, c are the three degrees of freedom for translational motion or rotational motion.

EPI data processing

The motion corrected images were coregistered with the high-resolution anatomical image, and then normalized to the Montreal Neurological Institute (MNI) standard template using FSL. Gaussian smoothing with an 8 mm kernel was then applied to the normalized images. Smoothing can effectively reduce thermal noise which is spatially uncorrelated, but has limited effects on physiological noise, which is partially correlated in space (Triantafyllou et al. 2006). The smoothed normalized images were input into a Matlab (The Mathworks, Inc, Natick, MA, USA) script to calculate the noise and temporal signal-to-noise ratio (SNR) of the resting state fMRI signal. The script uses quadratic detrending to remove the slowly varying MRI scanner drift for the time series of each voxel and then computes the standard deviation of the voxel-wise time course as the temporal noise. The temporal noise derived from the smoothed images is dominated by physiological noise. The physiological noise, however, is proportional to the amplitude of the MRI signal (Kruger and Glover 2001), which is proportional to the sensitivity of the receive coil if a phased array coil is used (Roemer et al. 1990). Therefore, the physiological noise can be dramatically influenced by the sensitivity of the coil, which could vary dramatically in space. The sensitivity is usually high near the coil and decay with distance. As a result, those voxels closer to the coil tend to have both higher signal and higher noise because physiological noise is proportional to the signal strength. To remove this confounding effect for multi-subject comparisons, the temporal signal-to-noise ratio (TSNR) was used to compare the two subject groups instead of the absolute value of noise. TSNR was computed on a voxel-wise basis, defined as the mean signal of the time series divided by the standard deviation of the time series (Triantafyllou et al. 2005). Because TSNR is a ratio, the linear effect of coil sensitivity in signal and physiological noise cancels out.

Statistics

The TSNR image of both SZ patients and controls were input into SPM8 (Wellcome Department of Cognitive Neurology, London, UK) and a two-sample *t*-test was performed. The total movement was used as a covariate in the *t*-test. We used a statistical threshold of $P<0.001$ (uncorrected) with a cluster size of >100 voxels for the final results. Clusters were identified for the statistical results. For each cluster, information of up to three separate local maxima (>8 mm apart) was extracted.

DTI and tract-based spatial statistics (TBSS)

The DTI data were first processed with the FDT toolbox of FSL (http://www.fmrib.ox.ac.uk/fsl/) to correct artifacts induced by head motion and eddy currents. All image volumes were registered to the first b0 image via an affine transformation. The diffusion tensor was also computed using the FDT toolbox along with the FA map. The FA maps were exported to the

pipeline of TBSS analysis. In TBSS, the target was chosen to be FMRIB58_FA standard image space; the mean FA skeleton was extracted from all the subjects. Number of permutations= 5000. The corrected p-value image was used in comparison with the results of TSNR, and the threshold statistics image ($p<0.05$) was thickened for better visualization.

Results

Temporal signal-to-noise ratio (TSNR) maps from one representative control subject are shown in Fig. 1. Figure 1a is the TSNR map without smoothing and normalization, showing higher TSNR in peripheral regions because of the higher coil sensitivity. Because the physiological noise correlates in space while thermal noise does not, the thermal noise was significantly reduced and the physiological noise became dominant after smoothing with an 8 mm Gaussian kernel. The overall SNR increased more than three times. The TSNR map shows very good contrast between the white matter and gray matter/CSF because the physiological noise is much lower in the white matter (Fig. 1b).

Head motion information is presented in Fig. 2. Figure 2a displays the mean values and standard deviations of total selected volumes for SZ and NC subjects. On average, approximately 10 % of the total volumes were removed from the TSNR analysis. The total number of volumes selected for computing TSNR was approximately equal for both groups. Figure 2b compares translational motion and rotational motion for the retained volumes. The translational motion of the SZ group is 0.0527 ±0.0307 mm and the translational motion of the NC group is 0.0529 ± 0.0263 mm. While the SZ group showed slightly higher rotational motion (0.0396±0.0250 mm vs. 0.0348± 0.0121 mm), this was not statistically significant ($p=0.386$). The standard deviation of the motion was slightly higher for SZ.

The statistical results of the two-sample *t*-test of TSNR between SZ patients and controls are displayed in Fig. 3. The TSNR difference between the two groups is widespread and contiguous. The difference is exclusively in the white matter, with controls showing higher TSNR values. Distinct voxels are clustered in several regions including temporal lobe, frontal lobe, and cerebellum, and spotted in major white matter tracts such as the corpus callosum, internal capsule, uncinate fasciculus, and superior longitudinal fasciculus. The distribution of these regions exhibits some degree of inter-hemispheric symmetry. With the same criteria, no region showed statistically higher TSNR for SZ.

TBSS showed wide-spread reduction of FA on major white matter tracts for schizophrenia subjects (Fig. 4). The regions showing lower FA values include the genu and body of the corpus callosum, the internal capsule, the external capsule, the fornix, the cingulum, the superior and inferior longitudinal fasciculus, the uncinate fasciculus, and the cerebellum. No region was found to have elevated FA values for SZ.

The distinctive regions from TSNR analysis shows some degree of overlap with the results from tract-based spatial statistics of fractional anisotropy values between the two groups, as illustrated in Fig. 5. Because the TSNR difference was on the volume while the TBSS difference was on the FA skeleton, a direct comparison is not possible. Table 1 lists the center coordinates of the clusters with higher TSNR for normal controls and the distances

between the center coordinates and TBSS differences. Most of the regions with higher TSNR in controls are aligned on the locations with higher FA values in controls such as the body of the corpus callosum and the internal capsule. Only one TSNR cluster in the cerebellum is quite apart from the TSBB difference. Most noticeably, not all the regions with higher FA for normal controls have higher TSNR, especially in the occipital lobe, where little difference was observed for TSNR.

Discussion

We examined functional and structural abnormality in white matter for schizophrenia by computing the signal fluctuation of resting state fMRI scans and fractional anisotropy from DTI scans. Both higher physiological noise and higher FA values were found in white matter for schizophrenia compared to normal controls. The regions of TSNR difference are partially aligned with the FA difference. The overlap lies mainly in the frontal lobe, which agrees with the result of an early study showing convergent evidence of deficits in functional connectivity between the frontal lobe and striatum from diffusion anisotropy and PET metabolic rate (Buchsbaum et al. 1998). Our findings may lead to a better understanding of the relationship between white matter functional activity and structural integrity.

A recent study focusing on gray matter reported a remarkable dissociation between the regions with anatomical and functional changes (Ren et al. 2013). Gray matter volume deficits from voxel-based morphometry were not significantly associated with the difference of amplitude of low-frequency fluctuations. As parallel research of structural-functional relationship in white matter, one of the important findings in this study is partial overlap between regions showing differential TSNR and those showing differential FA. The DTI analysis showed extensive differences between SZ and NC in the white matter. Since the two groups have similar motion, the difference is unlikely caused by motion artifacts and is consistent with a recent work of Lee et al. (Lee et al. 2013). The FA difference is mainly a reflection of alteration of white matter macromolecule structures, which might be related to axonal and myelination disruption (Beaulieu 2002; Davis et al. 2003), and consistent with prolonged T2. Recent work combining diffusion tensor spectroscopy and magnetization transfer rate suggested abnormalities in both axons and myelination in SZ in a region of the prefrontal cortex. Our result of elevated functional activity in white matter is likely due to higher metabolic rate in these regions, which Buchsbaum et al. presented a number of possibilities to explain the finding (Buchsbaum et al. 2007). Although our results cannot fully answer why functional activity is elevated in white matter, the partial overlap between TSNR difference and FA difference suggests that increased functional activity in white matter is unlikely to be related to the difference in white matter micro-structure, such as axon density, or results from possible neuronal damage. Therefore, inefficiency of neuronal transmission could be a plausible model for high white matter activity. Actually, electrophysiological and neuropsychological studies suggest abnormal synchronization of neural circuits in schizophrenia, which could be evidences of inefficient signal transmission (Innocenti et al. 2003; Spencer et al. 2003; Uhlhaas and Singer 2010). Based on our data, it is hard to quantify to what degree structural and functional changes are coupled in white

matter. However, based on the small overlap and larger scope of FA difference, it is unlikely that functional changes lead to microstructural changes.

An interesting finding is that the pattern of TSNR difference found here is very similar to that reported previously to be high in relative glucose metabolic rate in a PET study of schizophrenia (Buchsbaum et al. 2007). Although it is generally believed that at rest, physiological noise in MRI is highly related to metabolic activity, to our knowledge there is only one study attempting to relate these two measures (Wang et al. 2008). The good agreement of distinct regions in white matter with lower TSNR and those with higher glucose metabolic rate for SZ reported by Buchsbaum et al. suggests that TSNR in the white matter could be an additional measure of functional activity (Buchsbaum et al. 2007). Besides relative glucose metabolic rate increases, regional cerebral blood flow increases in white matter have also been previously observed in SZ (Pinkham et al. 2011). Both would be expected to lead to higher physiological noise, which is consistent with the results reported here. The difference in TSNR between the SZ and NC groups was widely distributed in the frontal lobe white matter, corpus callosum, white matter core of the temporal lobe, and cerebellum—all regions that have been shown previously to have white matter abnormalities in SZ (Kubicki et al. 2007).

The present study failed to detect significant TSNR differences in gray matter despite reports that SZ patients displayed lower metabolic rates and lower CBF (Buchsbaum et al. 2007; Pinkham et al. 2011), which should result in higher TSNR. The low sensitivity of the TSNR method in gray matter is probably due to the fact that gray matter is more inhomogeneous than white matter, in part due to the relative thinness of grey matter tissue; therefore smoothing is less effective. Also related to smoothing, gray matter is more contaminated by white matter as a result of smoothing because of the tissue thinness issue. Finally, there are more noise sources in gray matter such as low-frequency noise due to hardware imperfection, respiratory induced noise, and cardiac induced noise (Lund et al. 2006).

Because the above conclusions are drawn from the comparison of TSNR rather than the noise itself, it is necessary to consider whether there is any signal change in T2 weighted images for SZ. Lower TSNR can be caused by lower signal. However, it is not practical to compare the signal in our data as the image was acquired with a phased array coil. The sensitivity of a phased array coil varies significantly in space, resulting in large image non-uniformity. Given the same acquisition parameters, the image intensity of a T2-weighted image is mainly determined by the proton density and T2 relaxation value of the tissue. Previous studies have found prolonged water transverse relaxation time, T2, in the white matter of SZ compared to normal controls and there is little change in proton density (Andreasen et al. 1991; Du et al. 2012). Longer T2 leads to higher signal; hyperintensity in T2-weighted MRI images has been observed in the white matter for SZ (Sachdev and Brodaty 1999). If the physiological noise stays the same for the two groups, we should observe a high TSNR for SZ. Therefore, lower TSNR of SZ is unlikely caused by a change of signal size and can be solely attributed to elevated physiological noise.

An advantage of the TSNR analysis is that it does not require continuous time series. There are some limitations to our approach, though. For repeated scans of a fixed voxel in the brain, head movement can introduce significant signal change. Therefore, TSNR is very susceptible to head motion, as discussed in detail by Van Dijk et al. (Van Dijk et al. 2012). It is important to match the head motion between the two groups in comparing TSNR. This could be challenging in the study of some participant populations that have difficulty in keeping their heads still. Despite the similarity of physiological noise enhancement and increase of metabolic activity in schizophrenia patients, a quantitative relation between noise and metabolism can be difficult to obtain for a number of reasons. First, it is hard to separate physiological noise from other noise sources from resting state fMRI time series alone. Second, the relation between MRI signal variation and metabolic activity is far from clear. The signal change can be affected by many factors such as local vasculature, CBF, CBV, $CMRO_2$, and MRI acquisition parameters such as echo time. Another drawback of the approach is that similar to BOLD signal, TSNR can only be useful for a relative comparison. This is because the absolute value of TSNR has no meaningful relation with absolute metabolic rate.

In summary, we have employed TSNR to characterize the functional difference in white matter for SZ. Lower TSNR from resting state fMRI was found in distinct regions that have previously been reported to have higher relative glucose metabolic rates in PETstudies. A decrease of fractional anisotropy was observed diffusive over the brain. The two effects had some overlap but were not completely aligned, suggesting a dissociation of microstructural and functional abnormalities in white matter.

Supplementary Material

Refer to Web version on PubMed Central for supplementary material.

Acknowledgments

This work was supported by the National Institute of Mental Health (R01 MH074983 and R01 2MH074983 to WPH).

References

Andreasen N, Ehrhardt J, Swayze V, Tyrrell G, Cohen G, Ku JS, Arndt S. T1 and T2 relaxation times in schizophrenia as measured with magnetic resonance imaging. Schizophrenia Research. 1991; 5:223–232. [PubMed: 1760400]

Beaulieu C. The basis of anisotropic water diffusion in the nervous system - a technical review. NMR in Biomedicine. 2002; 15:435–455. [PubMed: 12489094]

Benes F. Emerging principles of altered neural circuitry in schizophrenia. Brain Research Brain Research Reviews. 2000; 31:251–269. [PubMed: 10719152]

Buchsbaum M, Tang C, Peled S, Gudbjartsson H, Lu D, Hazlett E, Downhill J, Haznedar M, Fallon J, Atlas S. MRI white matter diffusion anisotropy and PET metabolic rate in schizophrenia. Neuroreport. 1998; 9:425–430. [PubMed: 9512384]

Buchsbaum M, Buchsbaum B, Hazlett E, Haznedar M, Newmark R, Tang C, Hof P. Relative glucose metabolic rate higher in white matter in patients with schizophrenia. The American Journal of Psychiatry. 2007; 164:1072–1081. [PubMed: 17606659]

Camchong J, MacDonald A III, Bell C, Mueller B, Lim K. Altered functional and anatomical connectivity in schizophrenia. Schizophrenia Bulletin. 2011; 37:640–650. [PubMed: 19920062]

Davis K, Stewart D, Friedman J, Buchsbaum M, Harvey P, Hof P, Buxbaum J, Haroutunian V. White matter changes in schizophrenia: evidence for myelin-related dysfunction. Archives of General Psychiatry. 2003; 60:443–456. [PubMed: 12742865]

Ding Z, Newton A, Xu R, Anderson A, Morgan V, Gore J. Spatio-temporal correlation tensors reveal functional structure in human brain. PLoS ONE. 2013; 8:e82107. [PubMed: 24339997]

Du F, Cooper A, Cohen B, Renshaw P, Öngür D. Water and metabolite transverse T2 relaxation time abnormalities in the white matter in schizophrenia. Schizophrenia Research. 2012; 137:241–245. [PubMed: 22356802]

Du F, Cooper A, Thida T, Shinn A, Cohen B, Ongür D. Myelin and axon abnormalities in schizophrenia measured with magnetic resonance imaging techniques. Biological Psychiatry. 2013; 74:451–457. [PubMed: 23571010]

First, MB.; Spitzer, RL.; Miriam, G.; Williams, JBW. Structured clinical interview for DSM-IV-TR axis i disorders, research version, patient edition with psychotic screen (SCID-I/P W/PSY SCREEN). New York: Biometrics Research, New York State Psychiatric Institute; 2002.

Gawryluk J, Mazerolle E, D'Arcy R. Does functional MRI detect activation in white matter? A review of emerging evidence, issues, and future directions. Frontiers in Neuroscience. 2014; 8:239. [PubMed: 25152709]

Honea R, Crow T, Passingham D, Mackay C. Regional deficits in brain volume in schizophrenia: a meta-analysis of voxel-based morphometry studies. The American Journal of Psychiatry. 2005; 162:2233–2245. [PubMed: 16330585]

Hua K, Zhang J, Wakana S, Jiang H, Li X, Reich D, Calabresi P, Pekar J, van Zijl P, Mori S. Tract probability maps in stereotaxic spaces: analysis of white matter anatomy and tract-specific quantification. NeuroImage. 2008; 39:336–347. [PubMed: 17931890]

Innocenti G, Ansermet F, Parnas J. Schizophrenia, neurodevelopment and corpus callosum. Molecular Psychiatry. 2003; 8:261–274. [PubMed: 12660799]

Karlsgodt K, Niendam T, Bearden C, Cannon T. White matter integrity and prediction of social and role functioning in subjects at ultra-high risk for psychosis. Biological Psychiatry. 2009; 66:562–569. [PubMed: 19423081]

Kim S, Rostrup E, Larsson H, Ogawa S, Paulson O. Determination of relative CMRO2 from CBF and BOLD changes: significant increase of oxygen consumption rate during visual stimulation. Magnetic Resonance in Medicine. 1999; 41:1152–1161. [PubMed: 10371447]

Kruger G, Glover GH. Physiological noise in oxygenation-sensitive magnetic resonance imaging. Magnetic Resonance in Medicine. 2001; 46:631–637. [PubMed: 11590638]

Kubicki M, McCarley R, Westin C, Park H, Maier S, Kikinis R, Jolesz F, Shenton M. A review of diffusion tensor imaging studies in schizophrenia. Journal of Psychiatric Research. 2007; 41:15–30. [PubMed: 16023676]

Lee S, Kubicki M, Asami T, Seidman L, Goldstein J, Mesholam-Gately R, McCarley R, Shenton M. Extensive white matter abnormalities in patients with first-episode schizophrenia: a diffusion tensor imaging (DTI) study. Schizophrenia Research. 2013; 143:231–238. [PubMed: 23290268]

Lund TE, Madsen KH, Sidaros K, Luo W, Nichols TE. Non-white noise in fMRI: does modelling have an impact. NeuroImage. 2006; 29:54–66. [PubMed: 16099175]

Lynall M, Bassett D, Kerwin R, McKenna P, Kitzbichler M, Muller U, Bullmore E. Functional connectivity and brain networks in schizophrenia. The Journal of Neuroscience. 2010; 30:9477–9487. [PubMed: 20631176]

Ogawa S, Lee T, Kay A, Tank D. Brain magnetic resonance imaging with contrast dependent on blood oxygenation. Proceedings of the National Academy of Sciences. 1990; 87:9869–9872.

Pantano P, Baron J, Lebrun-Grandié P, Duquesnoy N, Bousser M, Comar D. Regional cerebral blood flow and oxygen consumption in human aging. Stroke. 1984; 15:635–641. [PubMed: 6611613]

Pfefferbaum A, Sullivan E, Hedehus M, Moseley M, Lim K. Brain gray and white matter transverse relaxation time in schizophrenia. Psychiatry Research. 1999; 91:93–100. [PubMed: 10515464]

Pinkham A, Loughead J, Ruparel K, Wu W, Overton E, Gur R, Gur R. Resting quantitative cerebral blood flow in schizophrenia measured by pulsed arterial spin labeling perfusion MRI. Psychiatry Research. 2011; 194:64–72. [PubMed: 21831608]

Raichle M, Gusnard D. Appraising the brain's energy budget. Proceedings of the National Academy of Sciences. 2002; 99:10237–10239.

Ren W, Lui S, Deng W, Li F, Li M, Huang X, Wang Y, Li T, Sweeney J, Gong Q. Anatomical and functional brain abnormalities in drug-naive first-episode schizophrenia. The American Journal of Psychiatry. 2013; 170:1308–1316. [PubMed: 23732942]

Ripke S, O'Dushlaine C, Chambert K, et al. Genome-wide association analysis identifies 13 new risk loci for schizophrenia. Nature Genetics. 2013; 45:1150–1159. [PubMed: 23974872]

Roemer P, Edelstein W, Hayes C, Souza S, Mueller O. The NMR phased-array. Magnetic Resonance in Medicine. 1990; 16:192–225. [PubMed: 2266841]

Sachdev P, Brodaty H. Quantitative study of signal hyperintensities on T2-weighted magnetic resonance imaging in late-onset schizophrenia. The American Journal of Psychiatry. 1999; 156:1958–1967. [PubMed: 10588411]

Shenton M, Dickey C, Frumin M, McCarley R. A review of MRI findings in schizophrenia. Schizophrenia Research. 2001; 49:1–52. [PubMed: 11343862]

Spencer K, Nestor P, Niznikiewicz M, Salisbury D, Shenton M, McCarley R. Abnormal neural synchrony in schizophrenia. The Journal of Neuroscience. 2003; 23:7407–7411. [PubMed: 12917376]

Triantafyllou C, Hoge R, Krueger G, Wiggins C, Potthast A, Wiggins G, Wald L. Comparison of physiological noise at 1.5 T, 3 T and 7 T and optimization of fMRI acquisition parameters. NeuroImage. 2005; 26:243–250. [PubMed: 15862224]

Triantafyllou C, Hoge R, Wald L. Effect of spatial smoothing on physiological noise in high-resolution fMRI. NeuroImage. 2006; 32:551–557. [PubMed: 16815038]

Uhlhaas P, Singer W. Abnormal neural oscillations and synchrony in schizophrenia. Nature Reviews Neuroscience. 2010; 11:100–113. [PubMed: 20087360]

Van Dijk K, Sabuncu M, Buckner R. The influence of head motion on intrinsic functional connectivity MRI. NeuroImage. 2012; 59:431–438. [PubMed: 21810475]

Wang H, Menezes N, Zhu M, Ay H, Koroshetz W, Aronen H, Karonen J, Liu Y, Nuutinen J, Wald L, Sorensen A. Physiological noise in MR images: an indicator of the tissue response to ischemia? Journal of Magnetic Resonance Imaging. 2008; 27:866–871. [PubMed: 18383248]

White T, Magnotta V, Bockholt H, Williams S, Wallace S, Ehrlich S, Mueller B, Ho B, Jung R, Clark V, Lauriello J, Bustillo J, Schulz S, Gollub R, Andreasen N, Calhoun V, Lim K. Global white matter abnormalities in schizophrenia: a multisite diffusion tensor imaging study. Schizophrenia Bulletin. 2011; 37:222–232. [PubMed: 19770491]

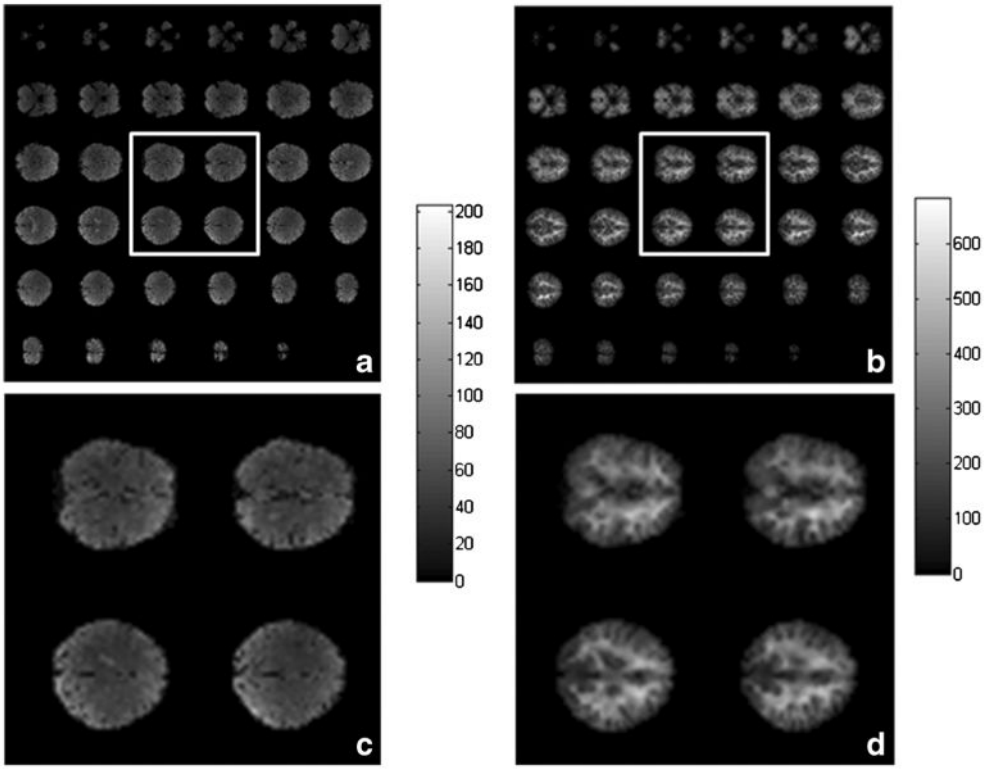

Fig. 1.

TSNR map of the resting state fMRI time series for a represented control subject. (**a**) oblique axial slices without smoothing; (**b**) with smoothing. Smoothing can reduce thermal noise but has little effect on the physiological noise. Four slices outlined in (*A*) and (*B*) are displayed in (*C*) and (*D*). Note that the white matter becomes prominent after smoothing

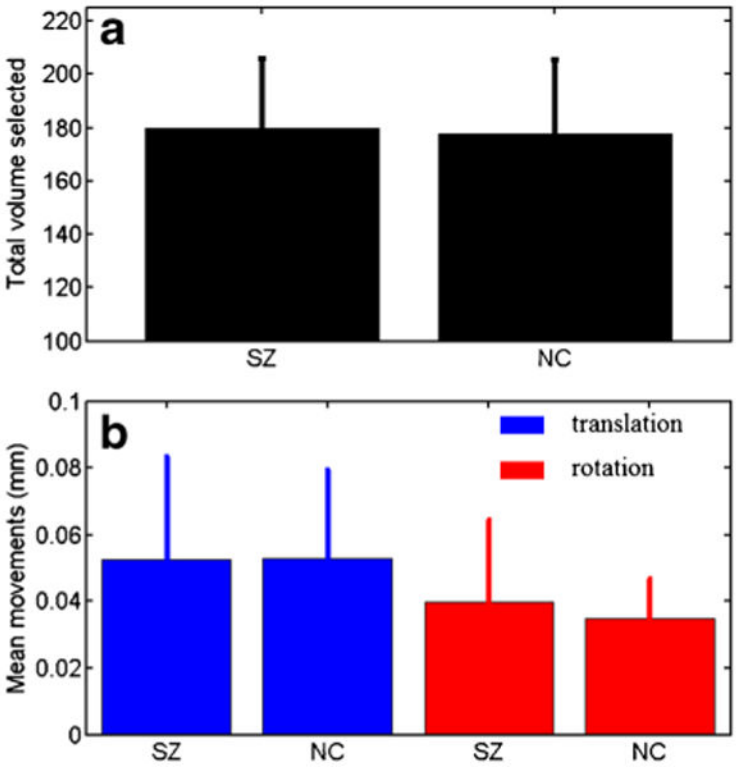

Fig. 2.

Comparison of motion information across SZ and NC subjects included in the study. (**a**) Total number of volumes selected for TSNR analysis for SZ and NC; (**b**) translational (*blue*) and rotational (*red*) movements for both SZ and NC. The translational and rotational movements were computed according to Eq. 2

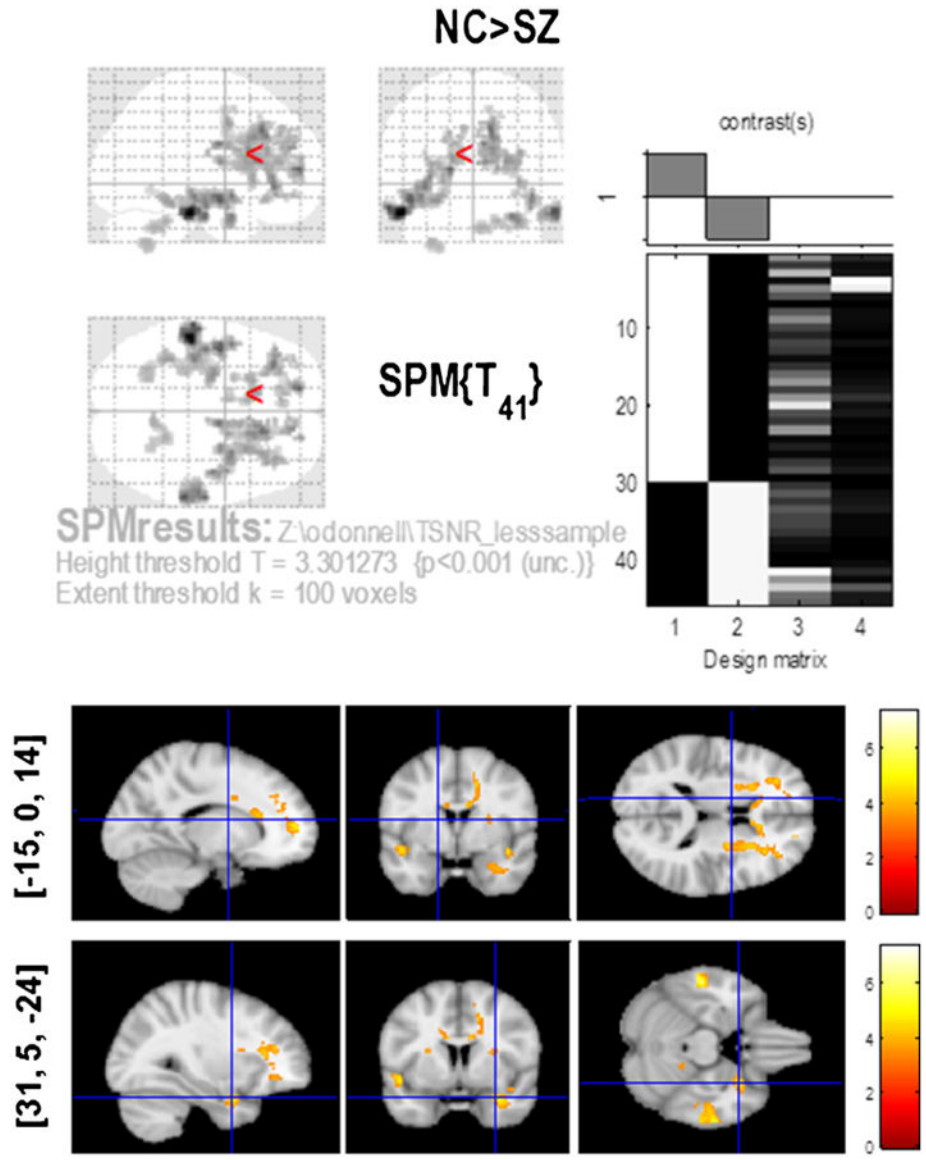

Fig. 3.

Statistical results from two-sample *t*-test of the TSNR maps between SZ and NC groups. Data are displayed in coronal planes 8 mm apart. The numbers on top indicate the location of slices in each hemisphere in MNI space. The statistical threshold is $p<0.001$ and cluster size> 100 voxels

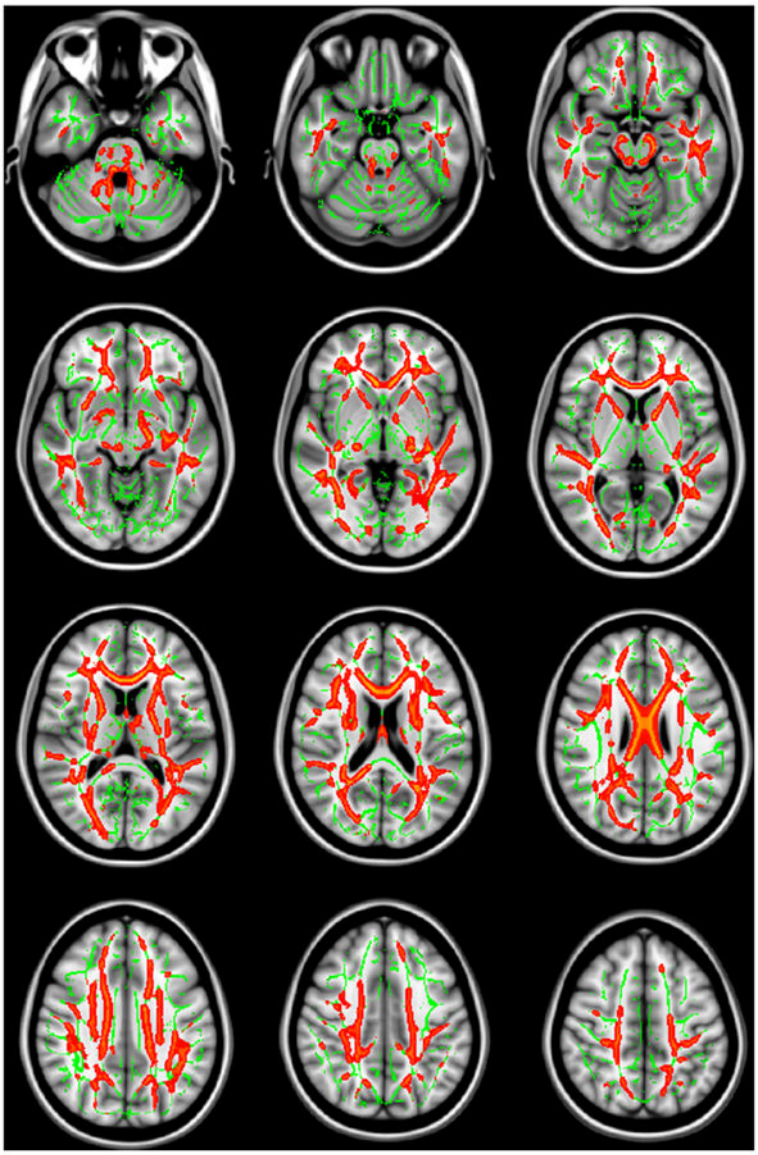

Fig. 4.

Results of TBSS analysis of FA values. Regions of significant FA reduction for SZ are shown in *red-yellow* with *p* value<0.05. The mean FA skeleton is displayed as *green lines*. The results are overlaid on the MNI template from Z=−30 mm to Z=47 mm. We applied 5000 permutations in the permutation-based nonparametric statistics. The p value was FWE corrected

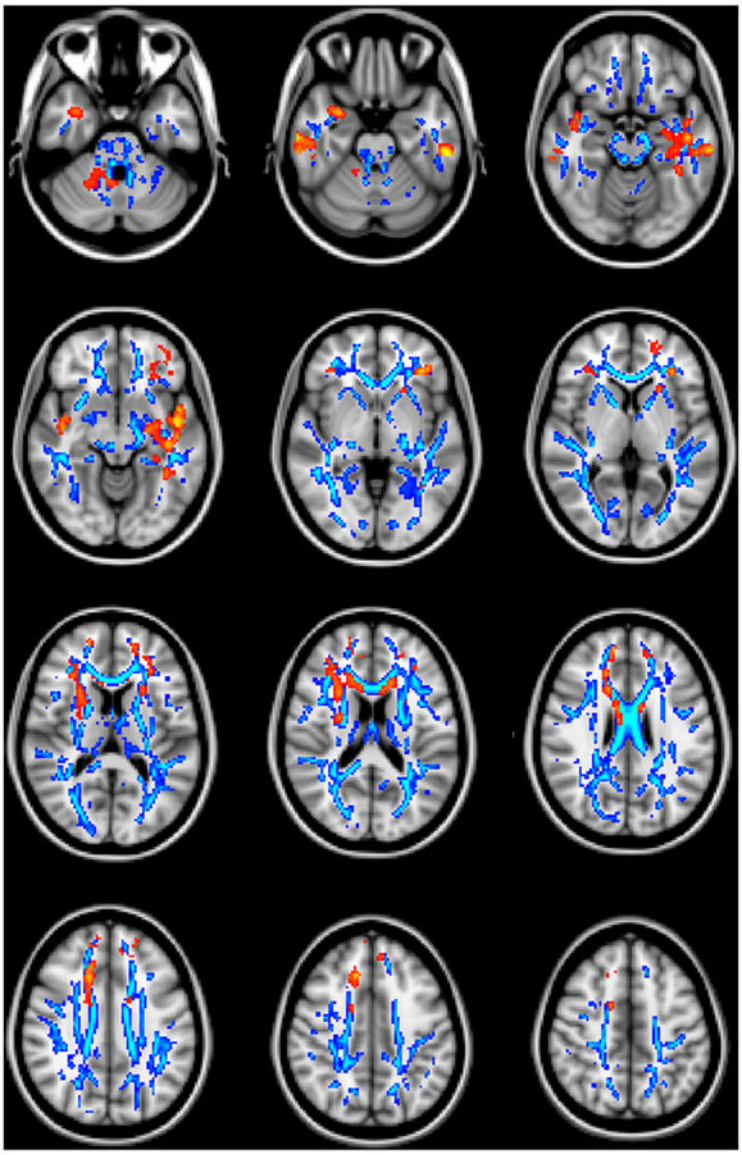

Fig. 5.

A comparison of SZ and NC group data for two sets of analyses. Data are displayed on the MNI template from Z=−30mm to Z=47 mm. Voxels that are significantly different between SZ and NC from the TSNR analysis (*red-yellow*, $p<0.001$ uncorrected to $p<0.05$ FEW corrected) overlaid on the results of the TBSS analysis (*blue-light blue*, $p<0.05$ to $p<0.01$)

Table 1

Clusters with higher TSNR for normal controls and their overlap with TBSS difference

Cluster location	Center coordinate (mm)	Number of voxels	Distance to TBSS (mm)	Effective radius (mm)
Cingulum (R)	[11, 14, 30]	1385	2.4	13.8
Inferior longitudinal fasciculus (L)	[−53, −18, −18]	1099	0	12.8
Inferior fronto-occipital fasciculus (L)	[−36 35–1]	318	1.4	8.5
Temporal lobe (R), unclassified	[57, −26, −23]	282	3.0	8.1
Corticospinal tract (R)	[16–50 −30]	181	0	7.0
Inferior longitudinal fasciculus (R)	[43–5–11]	138	3.7	6.4
Corpus callosum (body)	[−13 10 25]	136	1.4	6.4
Uncinate fasciculus (R)	[30, 4, −24]	132	4.5	6.3
Corticospinal tract (L)	[−30−58−42]	118	11.7	6.1
Anterior thalamic radiation (L)	[−23 14 5]	117	3	6.1
Forceps minor (L)	[−20, 52, 10]	107	1.4	5.9
Anterior thalamic radiation (L)	[−16 42 34]	104	1.4	5.8

The location of a cluster is derived from JHU white-matter tractography atlas by finding its closest white matter tract or structure (Hua et al. 2008). The center coordinate of a cluster is the mean MNI coordinates of the top three local maxima more than 8.0 mm apart in the cluster (depending on the cluster, number of local maxima can vary from 1 to >3). Distance to TBSS is computed as the shortest distance between any voxel in the FA skeleton that is significantly higher for normal controls to the center of a cluster. Effective radius refers to the radius of a sphere that contains the same number of voxels as the cluster